An Iterative Algorithm to Evaluate Multimodal *S*-Parameter-Measurements

H.-W. Glock and U. van Rienen

***Abstract*—Scattering-(S-)parameters are well established quantities to characterize RF-components both in theory and for measurement purposes. In spite of this, there are very few approaches to measure S-parameters in waveguide environments with more than a single propagating mode. In this paper we present a method for this purpose using a conventional single mode network analyzer, coaxial-waveguide adaptors to be calibrated within the procedure and waveguides of adjustable length. The most important step is the extraction of the devices S-parameters aimed for from the ensemble of single mode measurements. This is done by an iterative algorithm described in this paper.**

***Index Terms*—Measurement evaluation, multimode, S-parameter, waveguide.**

I. Introduction

The determination of S-parameters in a single mode (usually coaxial line) environment is a fundamental technique in rf measurement. So-called network analyzers (NWA) are used to measure the (2 × 2)-S-matrix of a two-port device. With appropriate adaptors they do this even for single-moded waveguides. The elimination of the adaptors influence from the result of the measurement is a standard problem in NWA measurements and commonly known as "calibration" or "de-embedding-problem" (see e.g. [1] for an overview of calibration approaches, [2] for a single mode procedure that has some similarities to our method). A special situation arises at signal frequencies high enough that higher order waveguide modes are able to propagate: though each mode is an independent port of the device there are no means to couple one mode individually over a broad frequency range and without disturbance of the others. The approaches in literature (e.g. [3] and references therein) to determine multimode S-parameters may be divided into two groups: 1) use of mode-selective couplers; 2) field pattern scanning with antenna arrays. The first approach relies on the assumption of ideal selectivity which is satisfactory only for small frequency bands. The second suffers either from small signals or from field disturbances due to the number of comparatively large antennas. Therefore we followed a different concept that utilizes waveguide-NWA-adaptors without any *a priori* demanded property. This implies the necessity to calibrate these adaptors within the procedure. The calibration uses a short and a waveguide of variable length; the measurement itself needs two calibrated adaptors and two adjustable waveguides. In either case the multimode S-parameters are to be extracted from a series of two-port S-parameters taken with different delay line lengths as shown in Fig. 1. The quantities directly observable depend in a nonlinear manner on *all* parameters to be measured; so their extraction needs a well suited algorithm presented here.

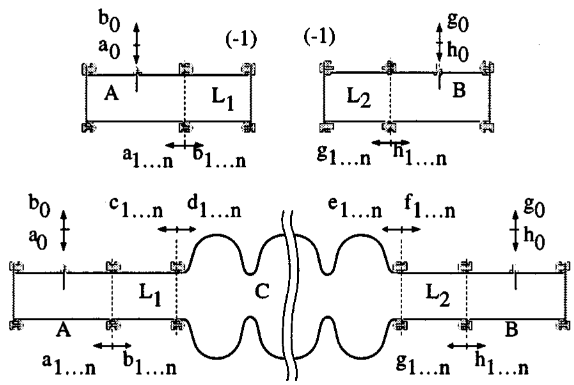

Fig. 1. Schematic drawing of setups used for adaptor calibration with delayed shorts (upper) and for measurement. Small letters denote the signals at all connection planes, index 0 corresponds to the coaxial lines, which have to be connected with a usual single mode network analyzer.

II. Theory of Measurement Setup

If we consider a setup with two adaptors A and B, a test device C and two connecting waveguides with lengths L_1 and L_2 (Fig. 1), we are able to write down all signals, related by appropriately defined S-matrices (ref. Fig. 1):

$$\begin{pmatrix} b_0 \\ \vec{b} \end{pmatrix} := \begin{pmatrix} A_{00} & \vec{A}^T \\ \vec{A} & \underline{\underline{A}} \end{pmatrix} \begin{pmatrix} a_0 \\ \vec{a} \end{pmatrix},$$

$$\begin{pmatrix} g_0 \\ \vec{g} \end{pmatrix} := \begin{pmatrix} B_{00} & \vec{B}^T \\ \vec{B} & \underline{\underline{B}} \end{pmatrix} \begin{pmatrix} h_0 \\ \vec{h} \end{pmatrix},$$

$$\begin{pmatrix} \vec{a} \\ \vec{d} \end{pmatrix} := \begin{pmatrix} 0 & \underline{\underline{E}}(L_1) \\ \underline{\underline{E}}(L_1) & 0 \end{pmatrix} \begin{pmatrix} \vec{b} \\ \vec{c} \end{pmatrix},$$

$$\begin{pmatrix} \vec{e} \\ \vec{h} \end{pmatrix} := \begin{pmatrix} 0 & \underline{\underline{E}}(L_2) \\ \underline{\underline{E}}(L_2) & 0 \end{pmatrix} \begin{pmatrix} \vec{f} \\ \vec{g} \end{pmatrix},$$

$$\begin{pmatrix} \vec{c} \\ \vec{f} \end{pmatrix} := \left(\underline{\underline{C}}_{11} \quad \underline{\underline{C}}_{12}\underline{\underline{C}}_{12}^T \quad \underline{\underline{C}}_{22} \right) \begin{pmatrix} \vec{d} \\ \vec{e} \end{pmatrix},$$

$$\begin{pmatrix} b_0 \\ g_0 \end{pmatrix} := \begin{pmatrix} \Gamma_1 & T \\ T & \Gamma_2 \end{pmatrix} \begin{pmatrix} a_0 \\ h_0 \end{pmatrix} \tag{1}$$

All the quadratic submatrices are $(n \times n)$-dimensional, n being the number of waveguide modes. For the waveguide of length L and the phase constants γ_j holds:

$$\underline{\underline{E}}(L) = \begin{pmatrix} e^{-\gamma_1 L} & 0 & 0 \\ 0 & \ddots & 0 \\ 0 & 0 & e^{-\gamma_n L} \end{pmatrix} \tag{2}$$

Manuscript received October 25, 1999.

The authors are with Institut für Allgemeine Elektrotechnik, Universität Rostock, Albert Einstein-Straße 2, D-18051 Rostock, Germany.

Publisher Item Identifier S 0018-9464(00)07146-6.

0018–9464/00$10.00 © 2000 IEEE

Using an additional abbreviation:

$$\underline{\underline{H}} := \begin{pmatrix} \underline{\underline{E}}(L_1) & 0 \\ 0 & \underline{\underline{E}}(L_2) \end{pmatrix} \begin{pmatrix} \underline{\underline{C}}_{11} & \underline{\underline{C}}_{12} \\ \underline{\underline{C}}_{12}^T & \underline{\underline{C}}_{22} \end{pmatrix} \cdot \begin{pmatrix} \underline{\underline{E}}(L_1) & 0 \\ 0 & \underline{\underline{E}}(L_2) \end{pmatrix} \tag{3}$$

one finds after the elimination of all signal quantities (comp. [4]) an equation that relates the overall (2×2)-S-matrix of the complete setup with all internal S-parameters of its components:

$$\begin{pmatrix} \Gamma_1 & T \\ T & \Gamma_2 \end{pmatrix} = \begin{pmatrix} A_{00} & 0 \\ 0 & B_{00} \end{pmatrix} + \begin{pmatrix} \vec{A}^T & 0 \\ 0 & \vec{B}^T \end{pmatrix} \underline{\underline{H}} \left[1 - \begin{pmatrix} \underline{\underline{A}} & 0 \\ 0 & \underline{\underline{B}} \end{pmatrix} \underline{\underline{H}} \right]^{-1} \cdot \begin{pmatrix} \vec{A} & 0 \\ 0 & \vec{B} \end{pmatrix} \tag{4}$$

The left hand side may be understood as a function of the two delay line lenghts L_1 and L_2 that is parameterized by the set-up's properties. It's the basic principle of the measurement to exploit different propagating constants of nondegenerated modes by varying waveguide lengths in a sequence of measurements to find these properties, i.e. the S-parameters. Therefore a—usually overdetermined—set of equations of the form (4) has to be solved either i) for the S-parameters of the ports (all A, B-quantities); this step is denoted as "calibration;" or ii) for the S-parameters of the $(2 \times n)$-port-device C; which we call here "measurement." The calibration requires a well known standard-object C, which is realized as a pair of shorts. This choice has first the advantage of easiest practical implementation and second it decouples the ports due to the vanishing transmission through C. This results in two separate equation systems of half the dimension of (4). Inversely, the ports A and B have to be known for the measurement step.

III. Principle of Numerical Procedure

The inverse matrix that appears in (4) induces a complicated nonlinear dependence on all individual S-parameters that leads to the failure of standard solution approaches. The key idea of our method is the expansion of the inverse matrix in a geometric series according to

$$(1 - \underline{\underline{M}})^{-1} = t(1 + \underline{\underline{M}} + \underline{\underline{M}}^2 + \underline{\underline{M}}^3 + \cdots). \tag{5}$$

This expansion is only valid if the geometric matrix series converges. It's a well known fact (comp. e.g. [5]) that this happens if all row- (and due to symmetry column-) value-sums of $\underline{\underline{M}}$ are smaller than 1:

$$\sum_{q=1}^{n} |M_{pq}| < 1 \quad \forall\, 1 \le p \le n \tag{6}$$

In [4] it's shown that even the weaker condition

$$\sum_{q=1}^{n} |M_{pq}| \le 1 \quad \forall\, 1 \le p \le n, p \ne p_0$$
$$\sum_{q=1}^{n} |M_{p_0 q}| < 1 \tag{7}$$

is sufficient under some assumptions about the structure of $\underline{\underline{M}}$, which are definetely fulfilled in case of completely filled matrices. This is of importance if objects without any internal power loss are considered.

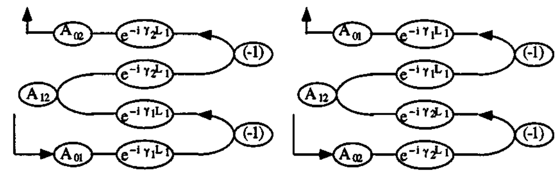

Fig. 2. An example for the interpretation of the geometric series found in (8) and (10): the two signal paths in the calibration setup that correspond to the term $2A_{01}A_{02}A_{12}e^{-2i(\gamma_1+\gamma_2)L_1}$.

The expansion (5) transforms (4) into the infinite sum

$$\begin{pmatrix} \Gamma_1 & T \\ T & \Gamma_2 \end{pmatrix} = \begin{pmatrix} A_{00} & 0 \\ 0 & B_{00} \end{pmatrix} + \begin{pmatrix} \vec{A}^T & 0 \\ 0 & \vec{B}^T \end{pmatrix} \underline{\underline{H}} \sum_{j=0}^{\infty} \left[\begin{pmatrix} \underline{\underline{A}} & 0 \\ 0 & \underline{\underline{B}} \end{pmatrix} \underline{\underline{H}} \right]^j \cdot \begin{pmatrix} \vec{A} & 0 \\ 0 & \vec{B} \end{pmatrix} \tag{8}$$

Physically the convergence of (8) is a consequence of decreasing signal amplitudes with increasing order of internal scattering. This condition is established even in the case of loss-free objects by the coupling to the external measurement system. The external ports are reflection-free by definition, so they carry power out of the system, coupling at least to one mode. This gives the physical interpretation of criterion (7).

Further discussion is simplified by restriction to the calibration step of port A. Then the equation equivalent to (4) is

$$\Gamma_1(L_1) = A_{00} - \vec{A}^T \underline{\underline{E}}^2(L_1)[\underline{\underline{1}} + \underline{\underline{A}}\,\underline{\underline{E}}^2(L_1)]^{-1}\vec{A} \tag{9}$$

and the geometric series expansion reads in the 2-mode case explicitly like

$$\begin{aligned} \Gamma_1(L_1) = A_{00} &- (A_{01}^2 e^{-2\gamma_1 L_1} + A_{02}^2 e^{-2\gamma_2 L_1}) \\ &+ (A_{01}^2 A_{11} e^{-4\gamma_1 L_1} + A_{02}^2 A_{22} e^{-4\gamma_2 L_1} \\ &+ 2A_{01}A_{02}A_{12} e^{-2i(\gamma_1+\gamma_2)L_1}) - \cdots \end{aligned} \tag{10}$$

Equation (10) expresses the measured input reflection $\Gamma_1(L_1)$ as linear combination of oscillations in length with well known wavenumbers. The coefficients are simple functions of the S-parameters searched for:

1	A_{00}	$\Rightarrow A_{00}$
$e^{-2i\gamma_1 L_1}$	$-A_{01}^2$	$\Rightarrow \pm A_{01}$
$e^{-2i\gamma_2 L_1}$	$-A_{02}^2$	$\Rightarrow \pm A_{02}$
$e^{-4i\gamma_1 L_1}$	$A_{01}^2 A_{11}$	$\Rightarrow A_{11}$
$e^{-4i\gamma_2 L_1}$	$A_{02}^2 A_{22}$	$\Rightarrow A_{22}$
$e^{-2i(\gamma_1+\gamma_2)L_1}$	$2A_{01}A_{02}A_{12}$	$\Rightarrow \pm A_{12}$

(11)

Furthermore (10) is a good representation in order to explain the physical relevance of (8) and (10), resp.. Each term describes the contribution of one distinct signal path as it's shown in Fig. 2. There two second order paths are indicated as sequence of: incidence (e.g. A_{01}), propagation (e.g. $e^{-i\gamma_1 L_1}$), reflection at the short ($r = -1$), propagation, scattering at the adaptor (A_{12}), propagation in the second mode ($e^{-i\gamma_2 L_1}$), again reflection at

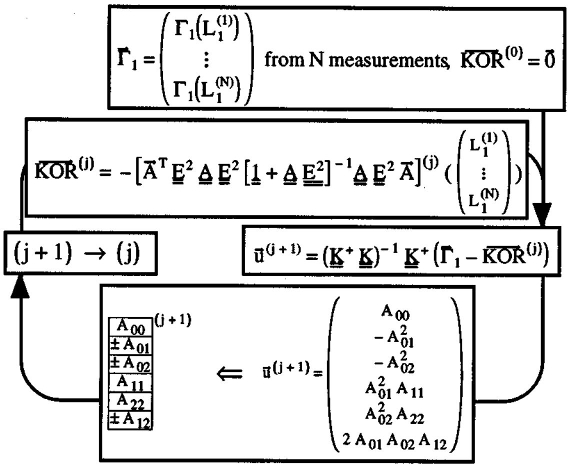

Fig. 3. Iteration scheme used for adaptor calibration as described above.

the short, propagation back to the adaptor, final coupling to the external system (A_{02}). In a similar manner all terms may be interpreted that are summed up in (4) and (9) in very compact expressions. If we would truncate the sum expansion using only terms printed in (10) a sufficiently large set of N measurements $\Gamma_1^{(j)}(L_1^{(j)})$ would allow us to solve for the terms indicated in the second column of (11) and in consequence for the S-parameters. We can do this applying the well-known scheme to find the best solution of overdetermined linear equation systems in the sense of least square:

$$\vec{u} = (\underline{\underline{K}}^+\underline{\underline{K}})^{-1}\underline{\underline{K}}^+\vec{\Gamma} \tag{12}$$

with (13) as shown at the bottom of the page. In this way the problem would be solved if there won't be an infinite number of signal paths with increasing number of internal reflections that have been neglected in (12), (13).

In order to incorporate their influence, a procedure was applied that consists of the following steps (comp. Fig. 3):

- Use (12) to find approximate start values of the S-parameters.
- Use them to calculate the approximative contribution of the higher order terms $\overrightarrow{KOR}$ to the measured reflection. Again they form an infinite geometric series. Thus they are expressed explicitly as inverse matrix.
- Subtract the higher order contribution from the measured data and once more determine an (improved) approximation of the S-parameters using (12), (13). (13) now holds the modified data $\vec{\Gamma} = (\vec{\Gamma}_1 - \overrightarrow{KOR}^{(j)})$.
- Repeat steps 2. and 3. until the calculated S-parameters converge which usually happens after a few loops.

In the case of a device measurement a more complicated procedure is needed which utilizes the same principle. The main differences are the use of three sets of measurement data (one transmission quantity $T(L_1, L_2)$, two reflection quantities $\Gamma_1(L_1, L_2)$, $\Gamma_2(L_1, L_2)$) each related to the respective reflection- or transmission-like S-parameters of the device C (14) and each connected with an approximative overdetermined linear equation system similar to (12) as shown in (14) at the bottom of the next page. As can be seen in (14), all parameters of C are found explicitly in the zeroth order term of the geometric series expansion (8), which makes situation somewhat easier compared to the calibration step where two orders were needed.

IV. Test and Application of the Algorithm

The procedure was tested in simulated experiments starting from an arbitrarily (within the restrictions of passivity and reciprocity) chosen set of S-parameters of a device C and/or of adaptors A, B used in the artificial setup. The external S-parameters one would measure if the experiment would be performed without any errors are calculated from (4), (9) resp. for a freely chosen set of delay line lengths. These data were fed back into the iterative procedure searching for the S-parameters originally given in order to test convergence and precision without error contributions of real experimental data.

The results of these tests were very encouraging. Table I shows a set of the 21 S-parameters of a device with two waveguide ports, each with three modes. In spite of start values found by total neglection of all higher scattering orders being partially about factors in error $(c11, c13, c22, \cdots)$ all S-parameters converge within four iterations to closest neighborhood of their "true" values. In order to quantify the deviation, an error function was defined:

$$\Delta s(\text{iter}) = \sum_{k \in \{11, 22, \cdots, 66\}} |c_k^{(\text{iter.})} - c_k^{(\text{true})}| \tag{15}$$

Fig. 4 shows the so-defined error found in simulated experiments with and without random noise added to the input "measurement" data. One observes an almost exponential decay of

$$\underline{\underline{K}} = \begin{pmatrix} 1 & e^{-2i\gamma_1 L_1^{(1)}} & e^{-2i\gamma_1 L_1^{(1)}} & e^{-2i\gamma_2 L_1^{(1)}} & e^{-4i\gamma_1 L_1^{(1)}} & e^{-4i\gamma_2 L_1^{(1)}} & e^{-2i(\gamma_1+\gamma_2) L_1^{(1)}} \\ \vdots & \vdots & \vdots & \vdots & \vdots & \vdots & \vdots \\ 1 & e^{-2i\gamma_1 L_1^{(N)}} & e^{-2i\gamma_1 L_1^{(N)}} & e^{-2i\gamma_2 L_1^{(N)}} & e^{-4i\gamma_1 L_1^{(N)}} & e^{-4i\gamma_2 L_1^{(N)}} & e^{-2i(\gamma_1+\gamma_2) L_1^{(N)}} \end{pmatrix}$$

$$\vec{u} = \begin{pmatrix} A_{00} \\ -A_{01}^2 \\ -A_{02}^2 \\ A_{01}^2 A_{11} \\ A_{02}^2 A_{22} \\ 2A_{01}A_{02}A_{12} \end{pmatrix}, \quad \vec{\Gamma} := \begin{pmatrix} \Gamma_1^{(1)}(L_1^{(1)}) \\ \vdots \\ \Gamma_1^{(N)}(L_1^{(N)}) \end{pmatrix} \tag{13}$$

TABLE I
SAMPLE S-PARAMETERS FOUND IN A SIMULATED EXPERIMENT

Par.	"Truth"/10^{-1}	start value/10^{-1}	4th iteration/10^{-1}
c11	1.4449 +1.3341 I	3.1847 -2.8648 I	1.4451 +1.3343 I
c12	1.3325 +0.12154 I	2.671 +1.9835 I	1.3322 +0.12143 I
c13	1.3581 -1.2674 I	0.3071 +0.31025 I	1.358 -1.2679 I
c14	0.20411 -0.92088 I	0.20222 -0.9146 I	0.20408 -0.92091 I
c15	0.85806 -0.26736 I	0.86926 -0.2760 I	0.8581 -0.26736 I
c16	0.20411 -0.92088 I	0.20389 -0.9171 I	0.20399 -0.92088 I
c22	-1.1618 -1.4336 I	-4.1269 -1.2024 I	-1.1613 -1.4339 I
c23	0.4031 -0.41991 I	0.21636 -0.7851 I	0.40329 -0.41974 I
c24	0.0066706 -0.3179I	0.00921 -0.3016 I	0.0067003 -0.3179 I
c25	0.75806 +0.96736 I	0.75313 +0.9824 I	0.75809 +0.96741 I
c26	0.40411 -0.62088 I	0.40474 -0.6113 I	0.40412 -0.62095 I
c33	1.3885 +2.6462 I	1.3138 +2.8975 I	1.3883 +2.6463 I
c34	-0.21326 -0.5999 I	-0.1976 -0.5829 I	-0.21309 -0.5999 I
c35	1.4581 -0.36736 I	1.471 -0.36093 I	1.4581 -0.3673 I
c36	-0.10411 +0.5209 I	-0.0977 +0.5366 I	-0.10416 +0.5208 I
c44	-2.319 -1.1083 I	-3.0121 -2.7701 I	-2.3188 -1.1073 I
c45	-0.65806 -1.2674 I	-2.132 -1.9579 I	-0.65702 -1.2662 I
c46	1.2041 -0.32088 I	1.0664 -1.2742 I	1.203 -0.31915 I
c55	1.4581 -0.46736 I	-2.0528 +0.5783 I	1.463 -0.46589 I
c56	2.1041 -0.92088 I	1.8415 -1.167 I	2.1039 -0.91918 I
c66	0.70411 +1.1209 I	0.68803 +1.2793 I	0.70508 +1.1195 I

the error with ideal input data that saturates at a certain point depending on the level of noise if there is any. Then the iteration result is trapped in the vicinity of the "truth." The method was applied to various objects in real measurements [4]. Due to lack of space and the difficulty of graphical representation, we restrict ourselves on the results found at a self-manufactured adaptor from koaxial line to a 78 mm diameter circular waveguide at a single frequency point with three waveguide modes able to propagate (Fig. 5). In Fig. 6. the coaxial input reflection as it was measured (dots) is displayed together with its value

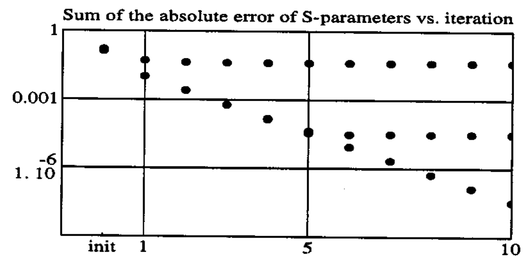

Fig. 4. Error of all S-parameters (logarithmic scale) according to (15) vs. iteration number with three different levels of artificial random noise added to the input data in a simulated experiment; point lines: top—noise of 1% of signal, middle—0.001% noise, lower with continuos slope—without noise. Points marked "init" correspond to the starting values found by neglecting higher order contributions to geometric series.

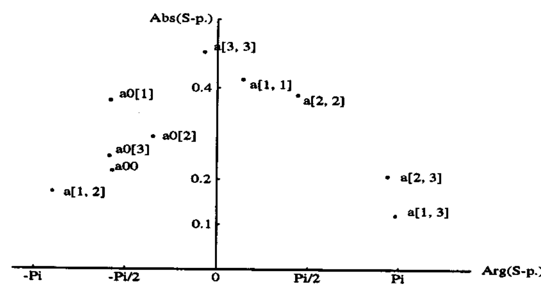

Fig. 5. Typical S-parameter set of an adaptor, found at 4.5 GHz, displayed in a Cartesian representation of the complex unit circle (value vs. argument). Index 0 denotes the coaxial line.

and argument calculated from the S-parameters found by our procedure (line). The correspondence of both is extremly good.

$$
\Gamma_1(L_1,L_2)\begin{array}{|c|c|c|}\hline e^{-2i\gamma_1 L_1} & A_{01}^2 C_{11} & \Rightarrow C_{11} \\ \hline e^{-2i\gamma_2 L_1} & A_{02}^2 C_{22} & \Rightarrow C_{22} \\ \hline e^{-2i\gamma_j L_1} & A_{0j}^2 C_{jj} & \Rightarrow C_{jj} \\ \hline e^{-i(\gamma_1+\gamma_2)L_1} & 2A_{01}A_{02}C_{12} & \Rightarrow C_{12} \\ \hline e^{-i(\gamma_j+\gamma_k)L_1} & 2A_{0j}A_{0k}C_{jk} & \Rightarrow C_{jk} \\ \hline \end{array}
$$

$$
T(L_1,L_2)\begin{array}{|c|c|c|}\hline e^{-i(\gamma_1 L_1+\gamma_1 L_2)} & A_{01}B_{01}C_{13} & \Rightarrow C_{13} \\ \hline e^{-i(\gamma_2 L_1+\gamma_1 L_2)} & A_{02}B_{01}C_{23} & \Rightarrow C_{23} \\ \hline e^{-i(\gamma_1 L_1+\gamma_2 L_2)} & A_{01}B_{02}C_{14} & \Rightarrow C_{14} \\ \hline e^{-i(\gamma_2 L_1+\gamma_2 L_2)} & A_{02}B_{02}C_{24} & \Rightarrow C_{24} \\ \hline e^{-i(\gamma_j L_1+\gamma_k L_2)} & A_{0j}B_{0k}C_{j(k+n)} & \Rightarrow C_{j(k+n)} \\ \hline \end{array}
$$

$$
\Gamma_2(L_1,L_2)\begin{array}{|c|c|c|}\hline e^{-2i\gamma_1 L_2} & B_{01}^2 C_{33} & \Rightarrow C_{33} \\ \hline e^{-2i\gamma_2 L_2} & B_{02}^2 C_{44} & \Rightarrow C_{44} \\ \hline e^{-2i\gamma_j L_2} & B_{0j}^2 C_{(j+n)(j+n)} & \Rightarrow C_{(j+n)(j+n)} \\ \hline e^{-i(\gamma_1+\gamma_2)L_2} & 2B_{01}B_{02}C_{34} & \Rightarrow C_{34} \\ \hline e^{-i(\gamma_j+\gamma_k)L_2} & 2B_{0j}B_{0k}C_{(j+n)(k+n)} & \Rightarrow C_{(j+n)(k+n)} \\ \hline \end{array} \qquad (14)
$$

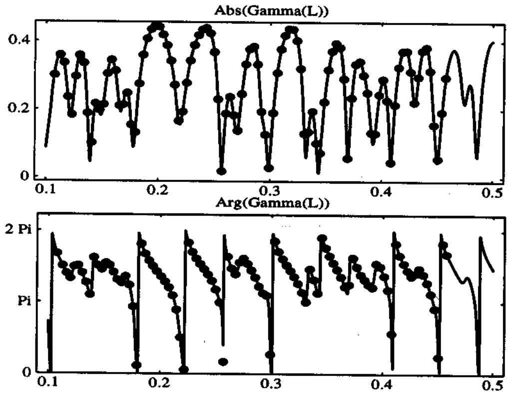

Fig. 6. $\Gamma(L)$, for test purposes calculated from the S-parameters from Fig. 5 (line) which were found in the iteration scheme and compared with measurement (dots).

V. Conclusions

It is possible to measure S-parameter in a multimode waveguide environment deducing them from data observable with single mode measurement devices. This can be done exploiting a system description in terms of infinite series of multiple scattering by an iteration scheme described above. Its convergence to the searched S-parameters within few iterations and its applicability to real measurement data are successfully demonstrated.

References

[1] R. A. Soares, P. Gouzien, P. Legaud, and G. Follot, "A unified mathematical approach to two-port calibration techniques and some applications," *IEEE Transactions on Microwave Theory and Techniques*, vol. 37, no. 11, pp. 1669–1673, Nov. 1989.

[2] v. Vaccaro, Coupling impedance measurements: An improved wire method, in Instituto Nazionale di Fisica Nucleare INFN/TC-94/023, Napoli, Nov. 1994.

[3] D. S. Levinson and I. Rubinstein, "A technique for measuring individual modes propagating in overmoded waveguides," *IEEE Transactions on Microwave Theory and Techniques*, vol. 14, no. 7, pp. 310–322, July 1966.

[4] H.-W. Glock, "Ein Verfahren für Streuparametermessungen an Hohlleiterstrukturen mit mehreren ausbreitungsfähigen Moden," Ph.D. Thesis, Universität Frankfurt/M, Germany, Nov. 1997.

[5] R. Courant and D. Hilbert, *Methoden der Mathematischen Physik*, 3rd ed. Berlin, Heidelberg: Springer-Verlag, 1968.